Reconfigurable Liquids Stabilized by DNA Surfactants

Bingqing Qian, Shaowei Shi,* Haiqiao Wang, and Thomas P. Russell

ABSTRACT: Polyelectrolyte microcapsules can be produced either by the layer-by- layer assembly technique or the formation of polyelectrolyte complexes at the liquid− liquid interface. Here, we describe the design and construction of DNA microcapsules using the cooperative assembly of DNA and amine-functionalized polyhedral oligomeric silsesquioxane (POSS-NH_2) at the oil−water interface. "Janus-like" DNA surfactants (DNASs) assemble in situ at the interface, forming an elastic film. By controlling the jamming and unjamming behavior of DNASs, the interfacial assemblies can assume three different physical states: solid-like, elastomer-like, and liquid-like, similar to that seen with thermoplastics upon heating, that change from a glassy to a rubbery state, and then to a viscous liquid. By the interfacial jamming of DNASs, the liquid structures can be locked-in and reconfigured, showing promising potentials for drug delivery, biphasic reactors, and programmable liquid constructs.

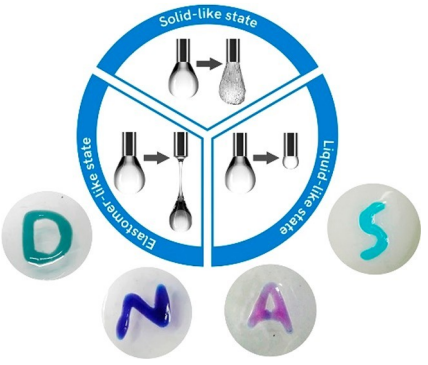

KEYWORDS: *DNA surfactants, interfacial assembly, jamming transition, microcapsules, structured liquids*

INTRODUCTION

The fabrication of polyelectrolyte microcapsules and the encapsulation of cargo in the microcapsules have attracted substantial attention, due to their promising applications in drug delivery, cosmetics, and food science.[1−4] Conventionally, these microcapsules are prepared by inducing complexation of two oppositely charged polyelectrolytes, for example by layer- by-layer (LbL) assembly, to form multilayers with unique stimuli-responsive properties.[5−7] However, the typical LbL assembly methods involve sequential deposition of polyelectrolyte layers onto a sacrificial template followed by the removal of the template, a multistep and time-consuming process. As an alternative to LbL, microdroplets can be used as "soft" templates to form polyelectrolyte microcapsules using a microfluidic process, based on the formation of polyelectrolyte complexes (PECs) at the oil−water interface of a droplet.[8,9] Nanoparticle−polyelectrolyte and protein−polyelectrolyte composite microcapsules can be prepared in a similar manner.[10−12] Lee and co-workers reported a more complex strategy for microcapsule fabrication, where the PECs are formed at the inner oil−water interface of water-in-oil-in-water (W/O/W) double emulsions followed by a spontaneous emulsion hatching.[13,14] However, in that case, one of the polyelectrolytes must be specifically synthesized or modified to ensure solubility in the oil phase, which complicates the preparation process and restricts wide application. Most efforts have focused on the generation of the microcapsules, while less attention has been paid to the assembly kinetics and aggregation of the polyelectrolytes at the interface, which play important roles in dictating the mechanical properties of the entire system.[15−19]

Here, a simple strategy for the fabrication of polyelectrolyte microcapsules is described by the cooperative assembly of polyelectrolytes and oligomeric/polymeric surfactants at the liquid−liquid interface. In this system, polyelectrolytes are dissolved in one liquid. By dissolving oligomeric/polymeric surfactants with complementary functionalization in the second liquid, "Janus-like" polyelectrolyte surfactants (PESs) form in situ at the interface, having hydrophilic polyelectrolyte chains anchored by hydrophobic oligomer/polymer tails. We note that the PESs described here are different from the well-studied polyelectrolyte−surfactant complexes that are formed in solution or in the solid state.[20−22] A key distinction is the generation of a supramolecular PES with an interfacial binding energy that is sufficiently strong to stabilize nonequilibrium liquid shapes, and to build the relationship between the assembly of PESs at the interface and macroscopic mechanical properties of assemblies.

As a proof-of-concept, we use a fascinating anionic polyelectrolyte, double stranded DNA, and an oil-soluble amine-functionalized polyhedral oligomeric silsesquioxane (POSS-NH_2, Supporting Information (SI) Figure S1), to generate DNA surfactants (DNASs) at the oil−water interface.

DNA, while being the universal carrier of hereditary information, also affords a versatile building block for guiding

the bottom-up fabrication of nanostructures and hybrid assemblies.[23−26] Due to the negatively charged phosphate groups, DNA presents a highly hydrophilic surface and is soluble in water and buffered aqueous solutions. POSS-NH_2, behaves as a surfactant, and can spontaneously assemble at the oil−water interface, changing the charge at the oil−water interface from negative (inherent to the oil−water interface) to positive.[27,28] By the electrostatic interactions between DNA and POSS-NH_2, DNASs form at the interface, allowing for the stabilization of microdroplets, producing an interfacial film with dynamic mechanical properties (Figure 1a). By tuning the

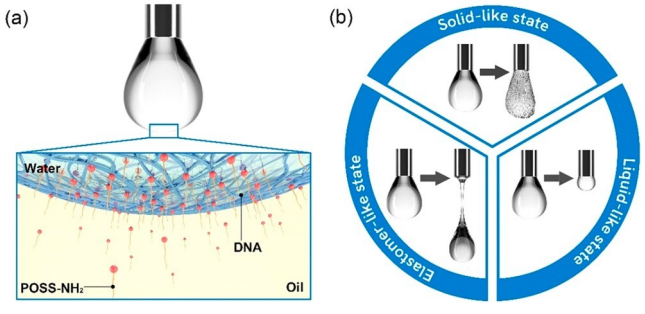

Figure 1. (a) The schematics of DNASs formation and assembly at the oil−water interface; (b) three physical states of interfacial assemblies constructed by DNASs.

concentration of DNA or POSS-NH_2, and the ionic strength or pH of the aqueous solution, the interfacial assemblies assume one of three physical states: solid-like, elastomer-like, and liquid-like, similar to that seen with thermoplastics upon heating, that change from a glassy to a rubbery and then a viscous liquid. (Figure 1b). The kinetic trajectory between the jammed and unjammed states of the interfacial assemblies can be directed in space and time by the reorganization of the DNASs. Using the emulsification or microfluidic technique, DNA microcapsules can be produced in a one-step process, with the ability to encapsulate a wide range of water-soluble materials, including biologically active materials, such as bovine serum albumin (BSA). By precisely controlling the dynamic mechanical properties of the assemblies, liquids can be reconfigured using a molding process, which are responsive to stimuli in their surrounding environment.[29,30]

RESULTS AND DISCUSSION

The interfacial kinetics of DNAS formation, assembly, and jamming at the oil−water interface was investigated by pendant drop tensiometry. As shown in Figure 2a, the pristine DNA ([DNA] = 0.1 mg/mL) is not interfacially active, due to its negative charge, with an interfacial tension of ~35 mN/m, essentially the same as that of the pure water−toluene system. With POSS-NH_2 [POSS-NH_2 = 0.1 mg/mL] dissolved in toluene against a pure water phase, the interfacial tension gradually decreases from 35 to 23 mN/m in 1200 s, showing that POSS-NH_2 behaves as a surfactant and assembles at the oil−water interface (SI Figure S1). With 0.1 mg/mL DNA dissolved in water and 0.1 mg/mL POSS-NH_2 dissolved in toluene, a further reduction in interfacial tension (γ) from ~35 to ~15 mN/m is observed in 1200 s, indicating the formation of DNASs at the interface. Interestingly, by reducing the droplet volume, an unusual phenomenon is observed where the droplet first elongates, with the formation of a neck between the droplet and needle. Capillary force decreases the diameter of the neck and gravitational force pulls the droplet down, stretching the region of the neck, forming a thin tubular structure which behaves like an elastomer (Figure 2c and SI Video S1). By increasing the POSS-NH_2 concentration to 0.5

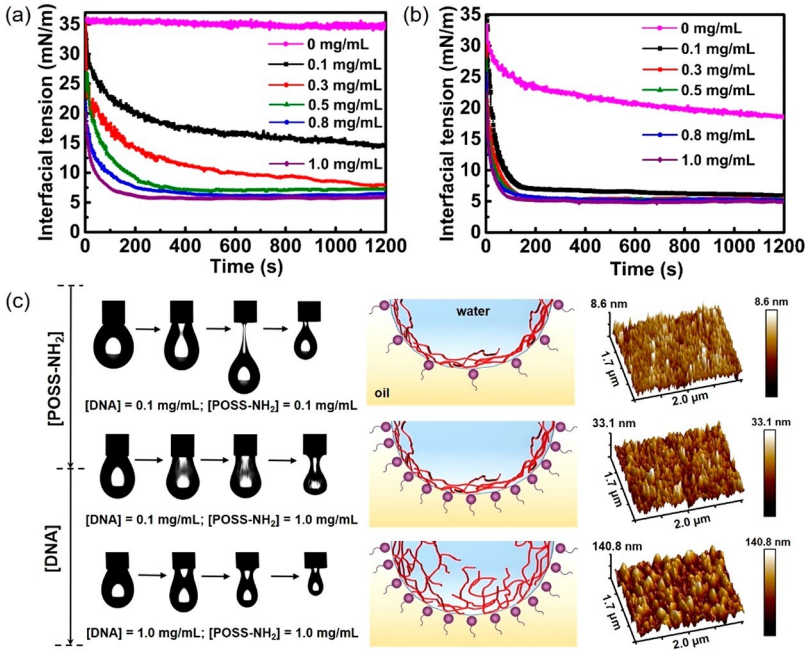

Figure 2. (a) Dynamic interfacial tension of the oil−water interface at different concentrations of POSS-NH_2, [DNA] = 0.1 mg/mL; (b) dynamic interfacial tension of the oil−water interface at different concentrations of DNA, [POSS-NH_2] = 1.0 mg/mL; (c) left: snapshots of droplet's morphology upon compression with different DNA or POSS-NH_2 concentrations; middle: schematic representations of the influence of DNA or POSS-NH_2 concentration on the mechanical properties of the interfacial assemblies; right: AFM images of 2D films self-assembled by DNAS with different DNA or POSS-NH_2 concentrations (assembly time: 1200 s).

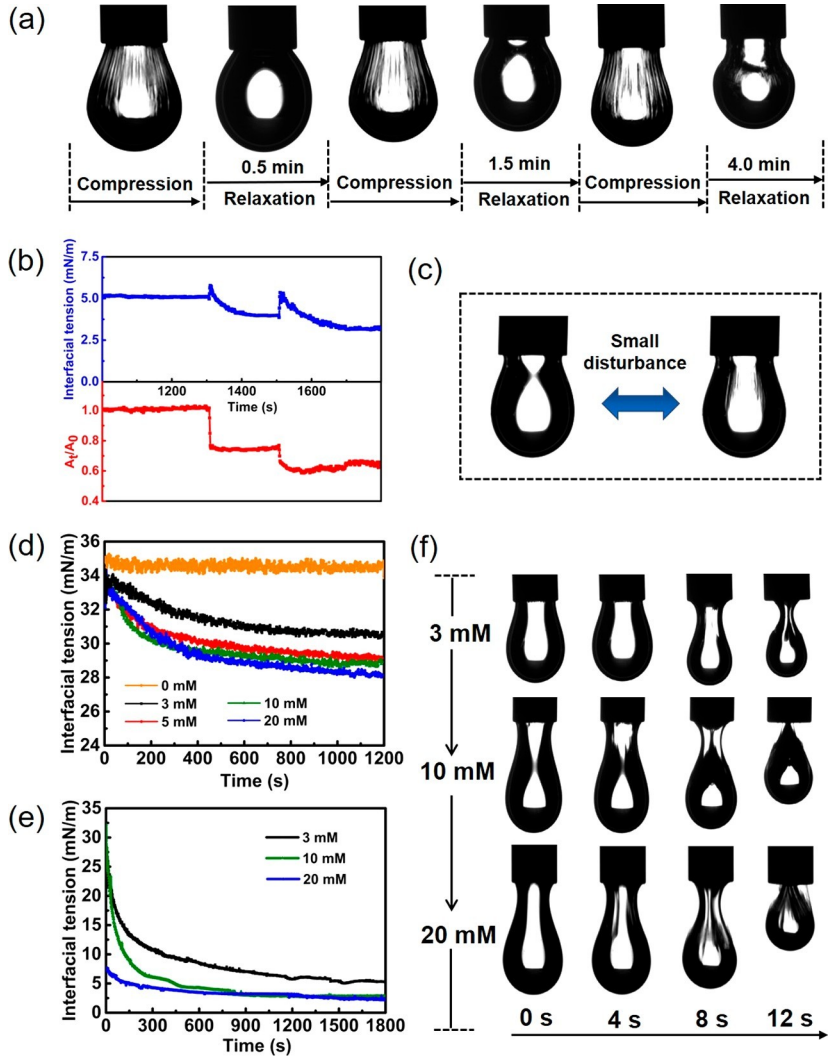

Figure 3. (a) Snapshots of droplet's morphology upon a repeated compression-relaxation experiment; (b) time evolution of interfacial tension and surface area in the first two compression-relaxation processes; (c) the unjamming-to-jamming transition of DNASs at the interface with a small disturbance after the first compression-relaxation process, [DNA] = 0.1 mg/mL, [POSS-NH_2] = 1.0 mg/mL; d) time evolution of interfacial
tension of the oil−water interface with different $MgCl_2$ concentrations, [DNA] = 0.8 mg/mL, [POSS-NH_2] = 0 mg/mL; e) time evolution of interfacial tension of the oil−water interface with different $MgCl_2$ concentrations, [DNA] = 0.8 mg/mL, [POSS-NH_2] = 1.0 mg/mL; (f) snapshots of droplet's morphology upon compression at different $MgCl_2$ concentrations, with DNAS assembled at the interface, [DNA] = 0.8 mg/mL, [POSS-NH_2] = 1.0 mg/mL.

mg/mL, the interfacial tension drops rapidly, reaching an equilibrium value of ~7.2 mN/m in 350 s. When compressing the droplet, the elongation behavior is reduced with the formation of wrinkles on the droplet surface, indicating the jamming of DNASs at the interface, causing a reduction in the mobility of the DNASs at the interface that now exhibits solid- like characteristics (SI Video S2). When the concentration of POSS-NH_2 is increased to 1.0 mg/mL, the equilibrium interfacial tension does not decrease in proportion but wrinkles develop immediately, upon very small compression, showing further enhanced mechanical strength of the assemblies (Figure 2c and SI Video S3). In view of this, we assume that, with the increasing concentration of POSS-NH_2 (the smallest cube-type molecular silica) in the oil phase, the number of POSS-NH_2 anchored to each DNA chain increases, making the interfacial assemblies become more solid-like. POSS-NH_2 acts as an interfacial "anchor" of the DNA network. At low POSS-NH_2 concentration, DNA chains at the interface are not anchored strongly, and respond to an external field,

such as compression and stretching, making the network to be adaptive. At higher POSS-NH_2 concentration, interfacial DNA network is anchored to the interface at multiple points, firmly fixing the DNA to the interface, prohibiting a response by modifying the assembly. This is further supported by increasing the pH of aqueous solution of DNA, where, with less protonated POSS-NH_2 at the interface, the responsiveness of DNA assemblies can be significantly enhanced, leading to the formation of the elastic assemblies (SI Figure S2 and SI Video S6).

Fixing the POSS-NH_2 concentration at 1.0 mg/mL while the DNA concentration is increased from 0.1 to 1.0 mg/mL, yields a completely different assembly behavior. As shown in Figure 2b, the dynamic and equilibrium interfacial tensions are almost the same in all cases, indicating the influence of the DNASs on the interfacial energy is similar. However, when compressing the droplet, the solid-like characteristics of the assemblies are gradually weaker. By increasing the DNA concentration to 0.8 mg/mL, wrinkles appear after a certain degree of compression

(SI Video S4). With a higher DNA concentration of 1.0 mg/ mL, an elongation of the droplet occurs first and wrinkles can only be observed at large compressions (Figure 2c and SI Video S5). This can be explained by the electrostatic repulsion between the DNA chains. As the concentration of DNA increases, more DNA chains will segregate to the oil−water interface. However, the increased electrostatic repulsion between DNA limits the contact between each DNA chain and POSS-NH_2, leading to a "bird nest"-type of assembly at the interface. Although the interface is fully occupied by DNASs, the effective contact area of each DNA chain with the interface decreases (SI Figure S4). Low effective contact area translates into a low degree of cross-linking in the DNA network at the interface, making the interfacial assemblies more elastic. In support of this argument, 2D films were prepared by transferring assemblies prepared on planar liquid interface at a fixed POSS-NH_2 concentration of 1.0 mg/mL and characterized by atomic force microscope (AFM), as is shown in Figure 2c and SI Figure S5. By increasing the DNA concentration from 0.1 to 1.0 mg/mL, the root-mean-square (RMS) surface roughness of the hydrophilic surface with DNA increases markedly from 3.25 to 18.5 nm, confirming the formation of "bird-nest"-type of assembly.

The reorganization of the DNASs was investigated by repeated compression-relaxation experiments where the concentrations of DNA and POSS-NH_2 were fixed to 0.1 and 1.0 mg/mL. As shown in Figure 3a, after the droplet is suspended for 1200 s and reaches an equilibrium state, the assemblies are compressed to solidify the interface by jamming the DNASs assembly. When wrinkling is observed, the compression is stopped. After 30 s, the wrinkles gradually disappear, indicating a relaxation of DNASs at the interface. With further compression, DNASs jam again and new wrinkles develop immediately. However, the wrinkles again relax after a longer time of 1.5 min. The assembly is compressed again and the wrinkles do not fully relaxe, instead, a deformation of the droplet is observed. From the time evolution of interfacial tension and surface area of the first two compression-relaxation processes, the reduction in the surface area leads to a decrease in the interfacial tension, indicating the areal density of the DNASs increases by a reorganization of the DNASs at the interface (Figure 3b). At sufficiently high DNASs coverages, the relaxed droplet can easily wrinkle with a small disturbance, such as a slight vibration (Figure 3c). Also, by increasing the DNA concentration to 0.8 mg/mL, the compression-relaxation results show a more rapid, and more times of relaxation (SI Figure S6), which is consistent with our argument that the effective contact area of each DNA chain with the interface plays an important role in dictating the relaxation behavior of DNASs and the mechanical properties of the resultant assemblies.

Ionic strength can dramatically affect the electrostatic forces in solution. In particular, nonspecifically bound divalent ions, for example, Mg^{2+}, can significantly mediate attractive inter- DNA forces, attenuating the electrostatic repulsive force between DNA chains.[31,32] By adding different concentrations of $MgCl_2$ into DNA aqueous solution against pure toluene, the interfacial tension is found to decrease gradually with the increasing salt concentration, indicating that the DNA becomes interfacially active by the screen of negative charges (Figure 3d). However, the binding energy is still not sufficient to withstand the compressive force when the interfacial area decreases and the interfacial assemblies show a liquid-like

behavior (SI Video S7). With POSS-NH_2 dissolved in toluene, DNASs form in situ and assemble at the interface, and the binding energy of the DNASs is enhanced. By increasing the salt concentration to 10 and 20 mM, pendant droplets show enhanced elongation behavior initially, and the interfacial tension decreases more rapidly (Figure 3e). When compress- ing, the solid-like nature of the interfacial assemblies becomes evident (Figure 3f and SI Video S8). POSS-NH_2 acts as an interfacial anchor for the DNA by the formation of the ion pairs along the DNA chain. With increasing salt concentration, the decrease in the number of negative charges on the DNA decreases the number of active sites for interaction with POSS- NH_2. This enhances the ability for the DNAS assemblies to reorganize at the interface in response to an applied external field, and, consequently, gravitational force can easily cause the droplet to elongate.

Based on the above, we find that, by varying the interactions between DNA and POSS-NH_2 at the interface, three physical states of interfacial assemblies can be achieved. Without POSS- NH_2 dissolved in the oil phase, although the interfacial activity of DNA can be enhanced by increasing the ionic strength of aqueous solution, the interfacial binding energy is low, resulting in assemblies that are liquid-like and do not jam. By dissolving POSS-NH_2 in the oil phase, DNASs form in situ at the interface, resulting in the formation of a DNA network in an elastomer-like unjammed state, that can be stretched by gravity without breaking. By interfacial compression, the unjammed assembly of DNASs can be driven into a solid- like jammed state, that can be relaxed by a reorganization of the DNASs.

Having achieved this level of control, large-area DNA films were prepared at the oil−water interface with DNASs.[33] As shown in Figure 4a, at low concentrations of DNA (0.8 mg/ mL) and POSS-NH_2 (1.0 mg/mL), a wrinkled film can be observed at the interface when removing the (top) oil phase.

The mechanical strength of the film can be significantly enhanced by increasing the number of interfacial anchors, that is, increasing the concentration of POSS-NH_2 to 10 mg/mL. Using tweezers, the interfacial film can easily be brawn-up from the interface in its entirety and stretched like an elastomer without damage (Figure 4b and SI Video S9). When the film is stretched under crossed polarized light, a birefringence is evident, which disappears after removing the tension, indicating DNA chains are partly orientated under tension (SI Figure S8).[34]

Before fabricating DNA microcapsules using a glass capillary microfluidic device, the effect of DNASs on Plateau−Rayleigh (PR) instabilities of water jets was investigated using the tensiometer in a flush mode, by forcing 0.8 mg/mL DNA aqueous solution into toluene containing 1.0 mg/mL POSS- NH_2 through a narrow capillary. As shown in Figure 4c−e and SI Video S10, in comparison to the breakup behavior seen with a pure water jetted into pure toluene, uniform droplets (absent any satellite droplets) are formed, yielding stable DNA microcapsules at the bottom of the cell (Figure 4d and SI Figure S9). During the generation of the microcapsules, tiny tubular structures connecting the droplets form, reflecting the elasticity of the assemblies at the interface, that rupture during stretching, leading to the formation of the microcapsules (Figure 4d,e). Clearly, the rapid assembly, formation and reorganization of the DNASs at the oil−water interface underpin this behavior, as discussed above.

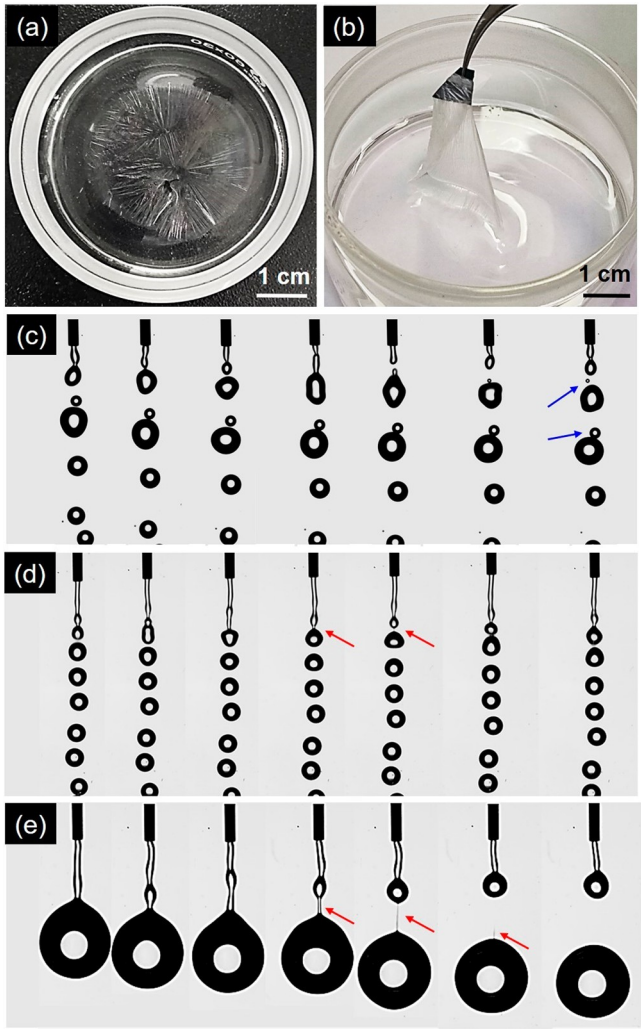

Figure 4. (a,b) Optical images of DNA films prepared at the oil− water interface with 1.0 (left) or 10 mg/mL (right) POSS-NH_2 dissolved in toluene and 0.8 mg/mL DNA dissolved in water (assembly time: 10 h); (c) high speed photography of a pure water jet falling in toluene; (d,e) high speed photography of an aqueous DNA solution with 0.8 (up) or 1.0 mg/mL (down) DNA falling in toluene solution containing 1.0 mg/mL POSS-NH_2. The initial jet diameter is 0.51 mm, and the flow rate is 2 mL/min.

Monodisperse water-in-oil emulsion drops were generated using a microfluidic device via the in situ formation and assembly of DNASs (Figure 5a). The as-prepared DNA microcapsules have a diameter of ~220 μm, with excellent stability and semipermeability, that can be further used for encapsulating a wide range of functional components such as proteins, enzymes, drug molecules, and inorganic nano- particles, to name a few (Figure 5b). Here we use fluorescein isothiocyanate bovine serum albumin (FITC-BSA) as a model cargo for the encapsulation. Confocal fluorescence microscopy image shows that BSA is contained within the droplets, with some segregated to the surface of the droplet due to the electrostatic interactions between negatively charged BSA and positively charged POSS-NH_2 (Figure 5c). After drying the microcapsules in

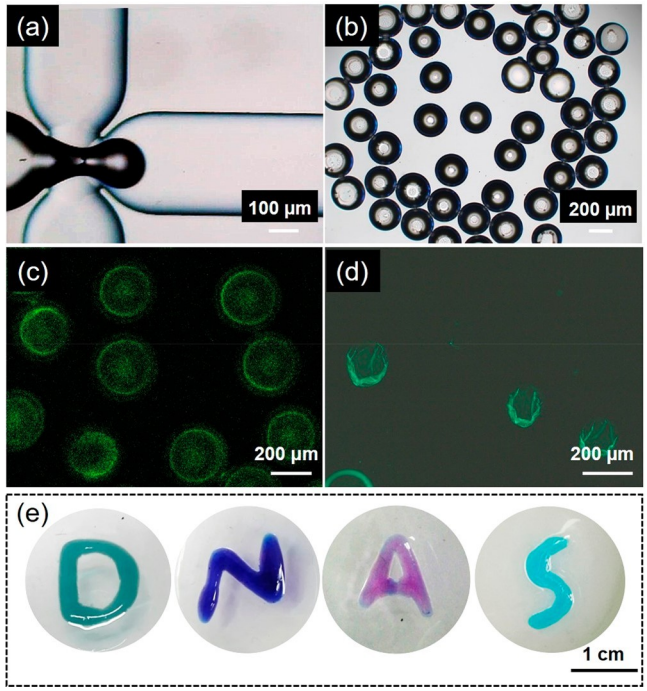

the air, the integrity of the capsule is maintained without breakup or significant collapse (Figure 5d), reflecting the excellent mechanical properties of the micro- capsules. Using a vortex mixer, water-in-oil or oil-in-water emulsions are also easily prepared (SI Figure S10). Finally,

Figure 5. (a) Optical microscope image of the glass capillary microfluidic device for the fabrication of DNA microcapsules; (b) optical microscope images of the produced DNA microcapsules, [DNA] = 0.8 mg/mL, [POSS-NH_2] = 1.0 mg/mL; (c) confocal fluorescence microscopy images of DNA microcapsules with FITC- BSA encapsulated in the droplets, [DNA] = 0.8 mg/mL, [POSS- NH_2] = 1.0 mg/mL, [FITC-BSA] = 0.03 mg/mL; (d) fluorescence microscope images of dried DNA microcapsules with FITC-BSA encapsulated in the droplets; (e) dyed liquid letters "DNAS" molded by the interfacial jamming of DNASs, [DNA] = 2.0 mg/mL, [POSS- NH_2] = 5.0 mg/mL.

using all-liquid molding, we demonstrate that liquids can be shaped into different structures and locked-in by the interfacial jamming of DNASs, and subsequently reconfigured by environmental stimuli such as pH (Figure 5e, SI Figure S11, and SI Video S11).

CONCLUSIONS

In summary, we have demonstrated the assembly, formation,
and jamming of the DNASs at the oil−water interface. By tuning the interactions between DNA and POSS-NH_2, the mechanical properties of the interfacial assemblies can be finely controlled, showing three different physical states: liquid-like, elastomer-like and solid-like. Upon application of external fields, for example, compression and stretching, the DNAS
assemblies can reorganize, relaxing in-plane stresses, ultimately controlling the macroscopic structural organization of the fluid phases. Using DNAS, DNA microcapsules can be produced in a one-step process using either emulsification or microfluidic techniques, with the ability to encapsulate materials. With solid-like DNAS interfacial assemblies, liquids can be molded,[30] providing a unique platform for the construction of programmable liquid devices for applications in biphasic chemical synthesis, chemical separations, and all-liquid electronics.[35,36]

AUTHOR INFORMATION

Corresponding Author

Shaowei Shi − *Beijing Advanced Innovation Center for Soft Matter Science and Engineering, Beijing University of Chemical Technology, Beijing 100029, China;* orcid.org/0000-0002-9869-4340; Email: shisw@mail.buct.edu.cn

Authors

Bingqing Qian − *Beijing Advanced Innovation Center for Soft Matter Science and Engineering, Beijing University of Chemical Technology, Beijing 100029, China*

Haiqiao Wang − *State Key Laboratory of Organic−Inorganic Composites, Beijing University of Chemical Technology, Beijing 100029, China;* orcid.org/0000-0003-3531-7393

Thomas P. Russell − *Beijing Advanced Innovation Center for Soft Matter Science and Engineering, Beijing University of Chemical Technology, Beijing 100029, China; Department of Polymer Science and Engineering, University of Massachusetts, Amherst, Massachusetts 01003, United States; Materials Sciences Division, Lawrence Berkeley National Laboratory, Berkeley, California 94720, United States;*

orcid.org/0000- 0001-6384-5826

ACKNOWLEDGMENTS

This work was supported by the National Natural Science Foundation of China (51903011) and Beijing Natural Science Foundation (2194083). T.P.R. was supported by the U.S. Department of Energy, Office of Science, Office of Basic Energy Sciences, Materials Sciences and Engineering Division under Contract No. DE-AC02-05-CH11231 within the Adaptive Interfacial Assemblies Towards Structuring Liquids program (KCTR16)

REFERENCES

(1) Peyratout, C. S.; Daehne, L. Tailor-Made Polyelectrolyte Microcapsules: From Multilayers to Smart Containers. *Angew. Chem., Int. Ed.* 2004, *43*, 3762−3783.

(2) De Geest, B. G.; De Koker, S.; Sukhorukov, G. B.; Kreft, O.; Parak, W. J.; Skirtach, A. G.; Demeester, J.; De Smedt, S. C.; Hennink, W. E. Polyelectrolyte Microcapsules for Biomedical Applications. *Soft Matter* 2009, *5*, 282−291.

(3) Volodkin, D. V.; Petrov, A. I.; Prevot, M.; Sukhorukov, G. B. Matrix Polyelectrolyte Microcapsules: New System for Macro- molecule Encapsulation. *Langmuir* 2004, *20*, 3398−3406.

(4) Ibarz, G.; Daﬁne, L.; Donath, E.; Möhwald, H. Smart Micro-and Nanocontainers for Storage, Transport, and Release. *Adv. Mater.* 2001, *13*, 1324−1327.

(5) Caruso, F.; Caruso, R. A.; Möhwald, H. Nanoengineering of Inorganic and Hybrid Hollow Spheres by Colloidal Templating. *Science* 1998, *282*, 1111−1114.

(6) Decher, G. Fuzzy Nanoassemblies: Toward Layered Polymeric Multicomposites. *Science* 1997, *277*, 1232−1237.

(7) Donath, E.; Sukhorukov, G. B.; Caruso, F.; Davis, S. A.; Mohwald, M. Novel Hollow Polymer Shells by Colloid-Templated Assembly of Polyelectrolytes. *Angew. Chem., Int. Ed.* 1998, *37*, 2201− 2205.

(8) Monteillet, H.; Hagemans, F.; Sprakel, J. Charge-Driven Co- Assembly of Polyelectrolytes Across Oil−Water Interfaces. *Soft Matter* 2013, *9*, 11270−11275.

(9) Kaufman, G.; Boltyanskiy, R.; Nejati, S.; Thiam, A. R.; Loewenberg, M.; Dufresne, E. R.; Osuji, C. O. Single-Step Microfluidic Fabrication of Soft Monodisperse Polyelectrolyte Microcapsules by Interfacial Complexation. *Lab Chip* 2014, *14*, 3494−3497.

(10) Kaufman, G.; Nejati, S.; Sarfati, R.; Boltyanskiy, R.; Loewenberg, M.; Dufresne, E. R.; Osuji, C. O. Soft Microcapsules with Highly Plastic Shells Formed by Interfacial Polyelectrolyte− Nanoparticle Complexation. *Soft Matter* 2015, *11*, 7478−7482.

(11) Kaufman, G.; Montejo, K. A.; Michaut, A.; Majewski, P. W.; Osuji, C. O. Photoresponsive and Magnetoresponsive Graphene Oxide Microcapsules Fabricated by Droplet Microfluidics. *ACS Appl. Mater. Interfaces* 2017, *9*, 44192−44198.

(12) Kaufman, G.; Mukhopadhyay, S.; Rokhlenko, Y.; Nejati, S.; Boltyanskiy, R.; Choo, Y.; Loewenberg, M.; Osuji, C. O. Highly Stiff yet Elastic Microcapsules Incorporating Cellulose Nanofibrils. *Soft Matter* 2017, *13*, 2733−2737.

(13) Kim, M.; Yeo, S. J.; Highley, C. B.; Burdick, J. A.; Yoo, P. J.; Doh, J.; Lee, D. One-Step Generation of Multifunctional Polyelec- trolyte Microcapsules via Nanoscale Interfacial Complexation in Emulsion. *ACS Nano* 2015, *9*, 8269−8278.

(14) Duan, G.; Haase, M. F.; Stebe, K. J.; Lee, D. One-Step Generation of Salt-Responsive Polyelectrolyte Microcapsules via Surfactant-Organized Nanoscale Interfacial Complexation in Emul- sions. *Langmuir* 2018, *34*, 847−853.

(15) Gao, C.; Donath, E.; Moya, S.; Dudnik, V.; Mohwald, H.
Elasticity of Hollow Polyelectrolyte Capsules Prepared by the Layer- by-Layer Technique. *Eur. Phys. J. E: Soft Matter Biol. Phys.* 2001, *5*, 21−27.

(16) Lulevich, V. V.; Radtchenko, I. L.; Sukhorukov, G. B.; Vinogradova, O. L. Deformation Properties of Nonadhesive Polyelectrolyte Microcapsules Studied with the Atomic Force
Microscope. *J. Phys. Chem. B* 2003, *107*, 2735−2740.

(17) Lulevich, V. V.; Radtchenko, I. L.; Sukhorukov, G. B.;
Vinogradova, O. L. Mechanical Properties of Polyelectrolyte Micro- capsules Filled with a Neutral Polymer. *Macromolecules* 2003, *36*,
2832−2837.

(18) Lulevich, V. V.; Andrienko, D.; Vinogradova, O. I. Elasticity of Polyelectrolyte Multilayer Microcapsules. *J. Chem. Phys.* 2004, *120*, 3822−3826.
(19) Vinogradova, O. J.; Andrienko, D.; Lulevich, V. V.; Nordschild, S.; Sukhorukov, G. B. Young's modulus of Polyelectrolyte Multilayers from Microcapsule Swelling. *Macromolecules* 2004, *37*, 1113−1117.
(20) Ober, C. K.; Wegner, G. Polyelectrolyte-Surfactant Complexes in the Solid State: Facile building blocks for self-organizing materials. *Adv. Mater.* 1997, *9*, 17−31.
(21) MacKnight, W. J.; Ponomarenko, E. A.; Tirrell, D. A. Self-Assembled Polyelectrolyte- Surfactant Complexes in Nonaqueous Solvents and in the Solid State. *Acc. Chem. Res.* 1998, *31*, 781−788.
(22) Zhou, S.; Chu, B. Assembled Materials: Polyelectrolyte− Surfactant Complexes. *Adv. Mater.* 2000, *12*, 545−556.
(23) Winfree, E.; Liu, F.; Wenzler, L. A.; Seeman, N. C. Design and Self-Assembly of Two-Dimensional DNA Crystals. *Nature* 1998, *394*, 539−544.
(24) Douglas, S. M.; Dietz, H.; Liedl, T.; Hogberg, B.; Graf, F.; Shih, W. M. Self-Assembly of DNA into Nanoscale Three-Dimensional Shapes. *Nature* 2009, *459*, 414−418.
(25) Liu, K.; Zheng, L.; Ma, C.; Gostl, R.; Herrmann, A. DNA-Surfactant Complexes: Self-Assembly Properties and Applications. *Chem. Soc. Rev.* 2017, *46*, 5147−5172.
(26) Kumar, B. P.; Patil, A. J.; Mann, S. Enzyme-Powered Motility in Buoyant Organoclay/DNA Protocells. *Nat. Chem.* 2018, *10*, 1154− 1163.
(27) Shi, S.; Qian, B.; Wu, X.; Sun, H.; Wang, H.; Zhang, H. B.; Yu, Z. Z.; Russell, T. P. Self-Assembly of MXene-Surfactants at Liquid- Liquid Interfaces: From Structured Liquids to 3D Aerogels. *Angew. Chem., Int. Ed.* 2019, *58*, 18171−18176.
(28) Liu, X.; Kent, N.; Ceballos, A.; Streubel, R.; Jiang, Y.; Chai, Y.; Kim, P. Y.; Forth, J.; Hellman, F.; Shi, S.; Wang, D.; Helms, B. A.; Ashby, P. D.; Fischer, P.; Russell, T. P. Reconfigurable Ferromagnetic Liquid Droplets. *Science* 2019, *365*, 264−267.
(29) Cui, M.; Emrick, T.; Russell, T. P. Stabilizing Liquid Drops in Nonequilibrium Shapes by the Interfacial Jamming of Nanoparticles. *Science* 2013, *342*, 460−463.
(30) Shi, S.; Liu, X.; Li, Y.; Wu, X.; Wang, D.; Forth, J.; Russell, T. P. Liquid Letters. *Adv. Mater.* 2018, *30*, 1705800.
(31) Baumann, C. G.; Smith, S. B.; Bloomfield, V. A.; Bustamante, C. Ionic Effects on the Elasticity of Single DNA Molecules. *Proc. Natl. Acad. Sci. U. S. A.* 1997, *94*, 6185−6190.
(32) Qiu, X.; Andresen, K.; Kwok, L. W.; Lamb, J. S.; Park, H. Y.; Pollack, L. Inter-DNA Attraction Mediated by Divalent Counterions. *Phys. Rev. Lett.* 2007, *99*, 038104.
(33) Sun, Z.; Feng, T.; Russell, T. P. Assembly of Graphene Oxide at Water/Oil Interfaces: Tessellated Nanotiles. *Langmuir* 2013, *29*, 13407−13413.
(34) Bravo-Anaya, L. M.; Macías, E. R.; Peŕez-Lopéz, J. H.; Galliard, H.; Roux, D. C. D.; Landazuri, G.; Carvajal Ramos, F.; Rinaudo, M.; Pignon, F.; Soltero, J. F. A. Supramolecular Organization in Calf- Thymus DNA Solutions under Flow in Dependence with DNA Concentration. *Macromolecules* 2017, *50*, 8245−8257.
(35) Liu, X.; Shi, S.; Li, Y.; Forth, J.; Wang, D.; Russell, T. P. Liquid Tubule Formation and Stabilization Using Cellulose Nanocrystal Surfactants. *Angew. Chem.* 2017, *56*, 12768−12772.
(36) Forth, J.; Liu, X.; Hasnain, J.; Toor, A.; Miszta, K.; Shi, S.; Geissler, P. L.; Emrick, T.; Helms, B. A.; Russell, T. P. Reconfigurable Printed Liquids. *Adv. Mater.* 2018, *30*, 1707603.